ANALYTICA CHIMICA ACTA 628 (2008) 80–86

available at www.sciencedirect.com

ScienceDirect

journal homepage: www.elsevier.com/locate/aca

# A electrochemiluminescence aptasensor for detection of thrombin incorporating the capture aptamer labeled with gold nanoparticles immobilized onto the thio-silanized ITO electrode

*Lanyun Fang*[a,b,c], *Zhaozi Lü*[a], *Hui Wei*[a,b], *Erkang Wang*[a,*]

[a] *State Key Laboratory of Electroanalytical Chemistry, Changchun Institute of Applied Chemistry, Chinese Academy of Sciences, Changchun 130022, Jilin, China*

[b] *Graduate School of the Chinese Academy of Sciences, Beijing 100049, China*

[c] *Ningbo Municipal Center for Disease Control and Prevention, Ningbo 315010, Zhejiang, China*

ARTICLE INFO

*Article history:*
Received 29 June 2008
Received in revised form
27 August 2008
Accepted 28 August 2008
Published on line 7 September 2008

*Keywords:*
Electrochemiluminescence (ECL)
Aptasensor
Thrombin
Gold nanoparticle

ABSTRACT

A novel electrochemiluminescence (ECL) aptasensor was proposed for sensitive and cost-effective detection of the target thrombin adopted an aptamer-based sandwich format. To detect thrombin, capture aptamers labeled with gold nanoparticles (AuNPs) were first immobilized onto the thio-silanized ITO electrode surface through strong Au–S bonds. After catching the target thrombin, signal aptamers tagged with ECL labels were attached to the assembled electrode surface. As a result, an AuNPs-capture-aptamer/thrombin/ECL-tagged-signal-aptamer sandwich type was formed. Treating the resulting electrode surface with tri-*n*-propylamine (TPA) and applying a swept potential to the electrode, ECL response was generated which realized the detection of target protein. Spectroscopy and electrochemical impedance techniques were used to characterize and confirm the fabrication of the ECL aptasensor. AuNPs amplification and smart sensor fabrication art were implemented for the sensitive and cost-effective detection purpose. Signal-to-dose curve excellently followed a sandwich format equation and could be used to quantify the protein, and the detection limit was estimated to be 10 nM. Other forms of thrombin such as β- and γ-thrombins had negligible response, which indicated a high specificity of α-thrombin detection. The aptasensor opened up new fields of aptamer applications in ECL domain, a highly sensitive technique, and had a promising perspective to be applied in microarray analysis.



## 1. Introduction

A rapid, effective and highly specific detection and quantification of biological substances are increasingly needed [1,2]. These biochemical materials can be determined by conventional binding methods with high degree of specificity such as antigen–antibody system, nucleic acid hybridization, avidin–biotin interaction and protein–ligand systems. In recent years, aptamers emerged as an attractive element in diverse analytical applications and bioassays [3–6].

Aptamers are short single-stranded nucleic acids that fold into well-defined three-dimensional structures in the conditions of their in vitro selection process called SELEX (systematic evolution of ligands by exponential enrichment)

* *Corresponding author*. Tel.: +86 431 85262003; fax: +86 431 85689711.
E-mail address: ekwang@ciac.jl.cn (E. Wang).

0003-2670/$ – see front matter © 2008 Published by Elsevier B.V.
doi:10.1016/j.aca.2008.08.041

[7]. Because of the high diversity of possible nucleotide sequence, aptamers can bind to their respective targets with high affinity, selectivity and specificity ranging from small molecules to proteins even whole cells [8–14]. Aptamer used as biorecognition element in analytical devices was extensively investigated for reasons of simple synthesis, good stability, easily chemical modification and wide applicability to extreme conditions [7,15]. A variety of detection methods were coupled to aptamer-based analysis including optical transduction [16], circular dichroism [17], electrochemistry [18–20], fluorescence [13,21], colorimetry [22], AFM [23], SPR [24] and quartz crystal microbalance [15].

ECL is inherently a highly sensitive and selective detection means which attracts considerable attention in pharmaceutical analysis, clinical diagnosis, environmental and food analysis and immunoassay as well as DNA detections, which were systematically reviewed by Richter [25] and Guilbault [26]. But tris(2,2′-bipyridine) ruthenium(II) [$Ru(bpy)_3^{2+}$]-based ECL immunoassay and DNA probe assays are not so popular, which used functional ruthenium complex as label since proteins and DNA cannot be directly detected by tris(2,2′-bipyridine) ruthenium(II). Previous work used commercial ECL labels, usually activated ruthenium NHS esters to modify biomacromolecules such as DNA and proteins [27–30]. The labels are very expensive, inconvenient and do not be sold without buying corresponding equipments (e.g. IGEN). Notice that there are some intrinsic distinct advantages of ruthenium labeling such as high stability, wide dynamic range, wide pH tolerance, easy multiple labeling without affecting bioactivities [27]. Extending ECL scope and exerting ECL superiority into bioanalysis are very helpful, valuable and of consequence. To our best knowledge, ECL or EIS aptasensor has been reported based on capture aptamers [31–33], but ECL approach for aptamer-based thrombin detection was seldom reported until now [34,35]. They used $Ru(bpy)_3^{2+}$-doped silica nanoparticle as DNA tags to get ECL signal enhancement. But, preparation of those tags was complicated and introduction of functional groups onto the surface of silica nanoparticles was tedious but necessary for labeling [36]. Still, the linkage of $Ru(bpy)_3^{2+}$ from silica nanoparticle was troublesome which would spoil the detection stability. In our work, we incorporate aptamer, the novel and efficient biorecognition element, and TBR ECL, the highly sensitive and favorable detection approach bridged by our self-synthesized activated $Ru(bpy)_3^{2+}$ NHS ester for protein detection. It is a simple, cost-effective and selective method. We just utilized an ITO-coated glass slide as assembly substrate, reversibly bound with a hollow PDMS layer on the ITO electrode surface to confine the area of ITO electrode, combined with self-assembly and AuNPs amplification techniques to fabricate a novel, smart, low-cost and sensitive ECL aptasensor for the detection of model protein, thrombin.

## 2. Experimental

### 2.1. Chemicals and materials

The oligonucleotides used in this study were purchased from Takara Biotechnology (Dalian) Co., Ltd. with the following sequences: 15-mer 5′SH-$(CH_2)_6$-GGTTGGTGTGGTTGG as capture aptamer and 29-mer 5′$NH_2$-$(CH_2)_6$-AGTCCGTGGTAGGGCAGGTTGGGGTGACT as signal aptamer. 3-Mercaptopropyltrimethoxysilane (MPTMS), tetrachloroauric acid ($HAuCl_4$), *N*-hydroxysuccinimide (NHS), thrombin, glutaraldehyde, bovine serum albumin (BSA), *N*,*N*′-dicyclohexylcarbodiimide (DCC), tri-*n*-propylamine (TPA), and anhydrous *N*,*N*′-dimethylformide (DMF) were purchased from Sigma–Aldrich. Human β-thrombin and γ-thrombin were purchased from Haematologic Technologies, Inc., (Essex Junction, VT, USA). Sodium citrate, methanol, ethanol, and acetone were bought from Beijing Chemical Corp. and were at least analytical reagent graded. All reagents were used as-received without further purification. ITO-coated glass (150-nM thick and $<15\,\Omega^{-2}$-resistant) was purchased from HIVAC Technology Co., Ltd. (Shenzhen, China). Sylgard 184 silicone elastomer and curing agent were obtained from Dow Corning (Midland, MI).

### 2.2. Apparatus and equipments

ECL is described as chemiluminescence produced directly or indirectly as a result of electrochemical reactions. It comprises electrochemical reactions on the electrode and light emitting process in the vicinity of the electrode. So, electrochemical reactions were carried out with a conventional three-electrode setup and monitored on a CH Instruments 832 Voltammetric Analyzer (CH Instrument Inc., USA). The ECL response was recorded on a Model BPCL Ultra-weak Luminescent Analyzer (Institute of Biophysics, Chinese Academy of Sciences) in which the photomultiplier tube was biased at −950 V. Working electrodes were ITO electrodes self-assembled layer-by-layer with different biomolecules. Ag/AgCl (saturated KCl) reference electrode and platinum counter electrode were used for all the electrochemical and ECL measurements.

The electrochemical impedance experiments (EIS) of the self-assemblies of biomolecules were performed in the presence of 1 mM $[Fe(CN)_6]^{3-/4-}$ (1:1) as the redox probe and the binding buffers (20 mM Tris–HCl, 140 mM NaCl, 5 mM KCl, and 1 mM $MgCl_2$) as supporting electrolyte. The spectra were measured by Autolab with PGSTAT 30 (Eco Chemie B.V., Utrecht, Netherlands) and with the aid of a frequency response analysis (FRA) system software under an oscillation potential of 5 mV over a frequency range of 10 kHz to 0.1 Hz. The impedance *Z* is expressed in term of a real ($Z_{re}$) and an imaginary ($Z_{im}$) component. UV spectra were recorded on a Cary 500 scan UV–vis–NIR spectrophotometer (Varian, Harbor City, CA). All measurements were performed at room temperature.

### 2.3. Preparation of oligonucleotide–AuNPs conjugate

AuNPs with a diameter of approximately 13 nM were prepared by the citrate reduction of $HAuCl_4$ in aqueous solution according to a well-known method [37]. In brief, 50 mL of aqueous solution containing 0.0167 g of $HAuCl_4$ was brought to a boiling reflux with stirring, and then 1.94 mL of 0.1 M sodium citrate solution was introduced quickly. After a fast color change, the solution was kept boiling for additional 20 min and left to cool to room temperature.

The synthesis of oligonucleotide–AuNPs conjugate was consulted to previous work [38] with necessary modification

by derivatizing 0.5 mL of the as-prepared AuNPs colloid (~17 nM) with 0.25 mL of the 15-mer capture aptamer (0.25 OD). After standing for 72 h at 25 °C, the nanoparticle conjugates were isolated by centrifugation for at least 15 min at 13,000 rpm to remove excess reagents. The supernatant was discarded, and the red pellet was redispersed in 500 μL of the 10 times-diluted binding buffer and kept at 4 °C. The resulting oligonucleotide–AuNPs conjugates were stable enough for at least 3 months without any aggregation.

### 2.4. Preparation of $Ru(bpy)_3^{2+}$ NHS ester-tagged oligonucleotide

The bis(2,2′-bipyridine)-4′-methyl-4-carboxybipyridine-ruthenium-*N*-succinimidyl-ester bis(hexafluorophosphate) (ECL probe) was prepared as described in our previous work elsewhere [39]. The $Ru(bpy)_3^{2+}$ NHS ester-tagged oligonucleotide was prepared with a slight modification according to the published procedures [40]. Briefly, 0.5 OD of 29-mer amino-modified signal aptamer dissolved in 500 μL PB buffer (pH 8.5), then 0.5 mg of the self-synthesized ECL probe was dissolved in 15 μL DMF and added to the oligonucleotide solution. The mixture was left to react in the dark overnight with delicate stirring. After the reaction finished, the ECL-tagged oligonucleotides were precipitated by addition of 50 μL of 3 M NaCl and 1.25 mL of cold, absolute ethanol. The mixture was kept at −20 °C for 1 h and then centrifuged for 15 min at 13,000 rpm. The supernatant was removed and the precipitate was washed three times with cold 70% ethanol to remove unreacted ECL probe. At last, the ECL-tagged oligonucleotide was dried in the air and finally dissolved in 100 μL of the binding buffer keeping at 4 °C until use.

### 2.5. Fabrication of ECL aptasensor with smart design of assembly procedure

ITO-coated glass slides were used as assembly electrodes owing to their stability, easy miniaturization and compatibility with microfabrication [41]. ITO glass slide with dimension of 4 cm × 1.2 cm was sonicated alternately with chemical detergent solution, deionized water, acetone and ethanol, each for 10 min to get clean ITO surface. After rinsing with ethanol and drying with $N_2$ stream, 1/3 part of the ITO electrode was immersed in 10% MPTMS methanol solution for 12 h. Through the bifunctional linker, MPTMS, the ITO surface was functionalized with a SH-rich self-assembled layer. Rinsed thoroughly with ethanol and dried, the modified part was reversibly bound to a punched PDMS layer which was prepared by curing the mixture of PDMS monomer and the curing agent (10:1) in an oven at 75 °C for 1.5 h. The effective electrode area was confined by the punched round hole with a diameter of 5 mm, which was used as reservoir for subsequent assembly. Afterward, a sandwich capture aptamer/thrombin/signal aptamer format was implemented to detect the protein.

#### 2.5.1. Attach the capture aptamer with AuNPs amplification

30 μL of oligonucleotide–AuNPs conjugates solution was introduced into the reservoir. The reservoir was then reversibly capped with another clean dry glass avoiding solution volatilization. After a 10-h self-assembly at 25 °C, uncover the cap and flush the reservoir with excessive deionized water and binding buffer followed by drying with $N_2$ stream.

#### 2.5.2. Bind the analyte with BSA-blocking

Standard thrombin sample containing 0.03 mg/mL BSA was added to the reservoir. BSA was used to reduce non-specific adsorptions. Then capped, incubated for 30 min at 37 °C, the electrode was flushed and dried.

#### 2.5.3. Bind the ECL-tagged signal aptamer

After the binding of thrombin, 20 μL of ECL-tagged oligonucleotide was added to the reservoir. Again, incubated at 37 °C for 30 min and then washed with copious amounts of deionized water and binding buffer solution, then dried under a $N_2$ stream.

#### 2.5.4. ECL detection

The generation of ECL response comprises electrochemical reactions of TPA and ECL label with a conventional three-electrode setup and a light emission process from the excited state to the ground state of the ECL label. The modified part of the ITO electrode was immersed in 50 mM TPA/0.1 M PB solution as working electrode. It was swept to an applied potential over the range of 0–1.3 V and the ECL signal was recorded on the instrument.

## 3. Results and discussion

### 3.1. Principle of the ECL aptasensor protocol

The schematic diagram of the principle of the present ECL aptasensor protocol was depicted in Fig. 1. The MPTMS-functionalized ITO electrode was prepared to immobilize AuNPs-labeled 15-mer capture aptamer through Au–S bond. AuNPs with large surface area can bind a large number of thiolated aptamers via the strong Au–S bond, leading to higher sensitivity [42]. After addition of target thrombin, the immobilized capture aptamers amplified with AuNPs were specifically combined with thrombin. When experienced with ECL-tagged 29-mer signal aptamer, a sandwich configuration of AuNPs-capture-aptamer/thrombin/ECL-tagged-signal-aptamer was formed. The two aptamers (15-mer and 29-mer) were reported to recognize different sites of thrombin and one aptamer binds to thrombin without serious influence on the other's binding to thrombin [20]. As the modified electrode was immersed in a TPA-containing electrolyte solution, ECL response emerged under an applied cyclic potential.

### 3.2. Characterization of oligonucleotide–AuNPs conjugate

AuNPs were chemically modified with 15-mer-thiolated capture aptamer as mentioned in Section 2.3. The surface coverage of aptamer to AuNPs has not been determined, but we have got much supportive information to confirm that many aptamers were attached to each individual AuNP. Firstly, Fig. 2 demonstrates the absorbance spectra of the as-prepared oligonucleotide–AuNPs conjugate. After modification, the

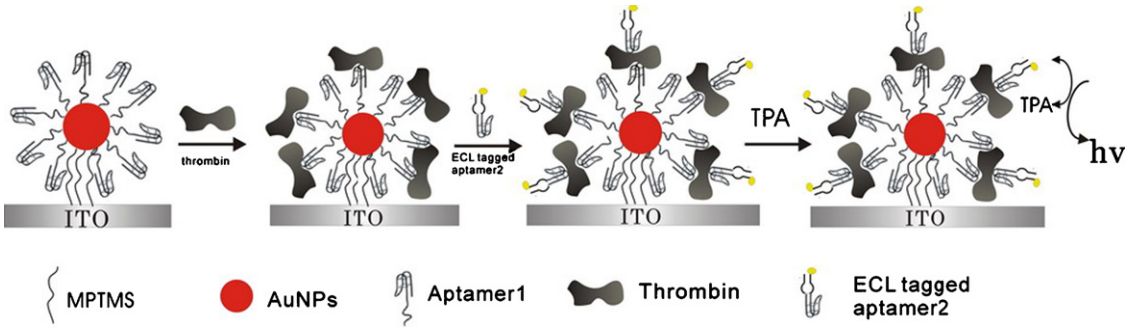


**Fig. 1 – The schematic diagram of fabrication of ECL aptasensor.**

characteristic surface plasmon band of monodispersed Au colloid at 519 nM does not change, but a new peak at 256 nm emerged. This is ascribed to the characteristic absorption band of DNA which validates the conjugation of aptamers to AuNPs. Secondly, we carried out another self-assembly procedure to immobilize capture aptamer without using AuNPs amplification, in which we used glutaraldehyde as cross-linking reagent to immobilize $NH_2$-aptamer onto amine-terminated ITO surface. The final results suggested that the performance of the latter route was very poor that we almost could not get any response. It was caused by the poor immobilization performance of capture aptamers to the substrate surface. So, it proved the successful attachment of AuNPs amplified aptamer to the electrode in a counter-side view.

### 3.3. *Characterization of ECL-tagged oligonucleotide*

The UV–vis absorbance spectra of the resulting 29-mer ECL-tagged signal aptamer dissolved in the binding buffer (300 μL) is demonstrated in Fig. 3. A characteristic absorption band at 258 nm is observed for oligonucleotide in the spectrum. And at visible region of 457 nm, a new peak appears. This reflects the characteristic metal-to-ligand electron transfer band of $Ru(bpy)_3^{2+}$ NHS ester, similar to $Ru(bpy)_3^{2+}$. The spectra are

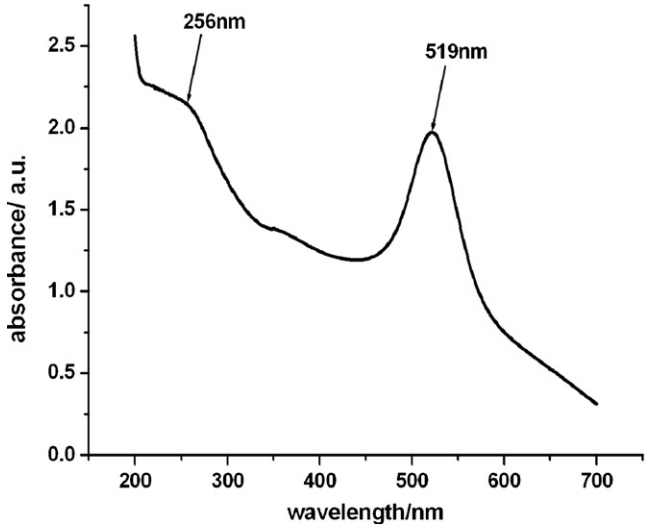


**Fig. 2 – The absorbance spectra of the resulting 15-mer oligonucleotide–AuNPs conjugate.**

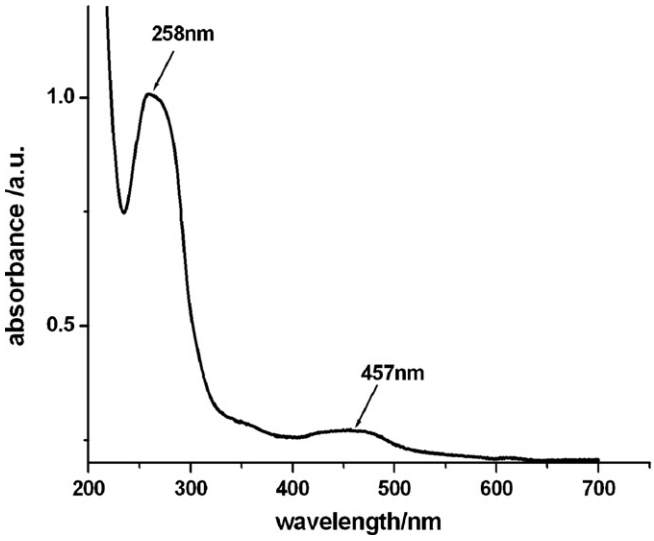


**Fig. 3 – The UV–vis spectra of the resulting ECL-tagged 29-mer oligonucleotide.**

in good agreement of previous works and confirm the successful labeling of the detection aptamer with ECL tag [29]. The concentration of the oligonucleotide (MW = 9410 g/mol) is quantified to be ~1.1 μM on the basis of UV absorbance value at 258 nm, and $A_{258\,nm}$/0.3 mL = 1.01, with a conversion factor of 33 μg $mL^{-1}$ $OD^{-1}$ [29]. So, the concentration of the ECL-tagged signal aptamer was at micromolar level and adequate for the sandwich assay.

### 3.4. *EIS monitoring of the fabrication of the ECL aptasensor*

EIS is an effective tool for probing the features of surface-modified and biomaterial-functionalized electrodes. The generous Randles model was used as the equivalent circuit for the fitted EIS measurements, in which the most decisive and directive parameter, electron-transfer resistance ($R_{et}$), reflects the changes of insulating features of electrode–electrolyte interface. Nyquist plot of EIS measurement shows a semicircle in the high-frequency region associated with resistance and capacitance elements in parallel while shows a straight line in the low-frequency region associated with mass transfer. In EIS, the value of $R_{et}$ equals the semicircle diameter.

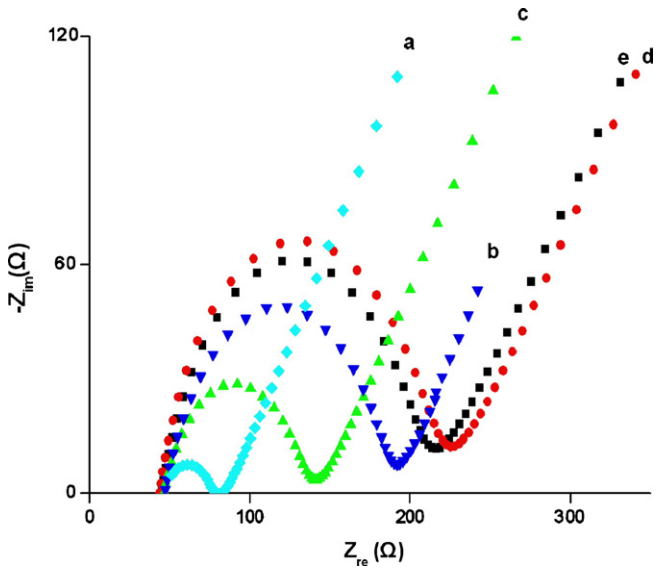


**Fig. 4 – Nyquist plot for the Faradaic impedance measurements of the modified ITO electrode by layer-by-layer self-assembly. (a) Bare ITO surface, (b) ITO\MPTMS surface, (c) ITO\MPTMS\AuNPs-aptamer1 surface, (d) ITO\MPTMS\AuNPs-aptamer1\thrombin surface, and (e) ITO\MPTMS\AuNPs-aptamer1\thrombin\ECL-aptamer2 surface. The spectra were recorded in the binding buffer containing 1 mM $[Fe(CN)_6]^{3-/4-}$ as redox probe, using a frequency of 10 kHz to 0.1 Hz under an oscillation potential of 5 mV.**

Our stepwise EIS measurements of the modified ITO electrode at different modification steps were carried out in the place of the PDMS reservoir as it ensures the same electrode area. When the stepwise modification finished, the reservoir was washed, dried and filled with probe solution for the EIS experiment. The results presented as Nyquist plot were well illustrated in Fig. 4. Significant differences in the EIS spectra were observed during the step-by-step modification. The bare ITO electrode exhibited a very small $R_{et}$ value of 65 Ω (Fig. 4a). Silanization of ITO surface with MPTMS generated an insulating layer on the electrode surface [43], which resulted in an increased electron transfer resistance (Fig. 4b). The $R_{et}$ value decreased a lot when AuNPs-labeled oligonucleotides were assembled on the electrode (Fig. 4c). This indicated the excellent conductive performance of AuNPs, which facilitate the electron transfer exceeding the repulsion interactions between the negative charged oligonucleotides and the probe ions and leading to a net decrease of electron transfer resistance. When further bound with thrombin, as expected, the electron transfer resistance elevated much as shown with Fig. 4d. This is the reflection of insulating features of proteins that block the electron transfer after formation of a thin layer onto the electrode.

Note that the assembly of thrombin introduced BSA-blocking that is a common and effective method to reduce non-specific adsorption in biospecific interactions. In a previous work, pretreatment with 0.01 mg/mL of BSA can dramatically reduced protein adsorptions [15,44] and in our work we adopt 0.03 mg/mL of BSA to block the sites of non-specific interactions. Furthermore, in our EIS measurements, preadsorption of BSA before binding of thrombin and binding of thrombin in the presence of BSA were carefully compared. It was found that the differences of $R_{et}$ values between ITO\MPTMS\Au-aptamer\BSA\thrombin-modified electrode and ITO\MPTMS\Au-aptamer\thrombin-modified electrode (in the presence of BSA) with ITO\MPTMS\Au-aptamer-modified electrode were almost the same. Besides, in the former case, $R_{et}$ value of ITO\MPTMS\Au-aptamer\BSA\thrombin-modified electrode increased compared with ITO\MPTMS\Au-aptamer\BSA-modified one. This indicated thrombin was successfully combined to the electrode surface. To reduce assembly steps and improve sensing efficiency, we performed BSA-blocking in the form of coexistence with target thrombin. So, in one word, according to the EIS results, thrombin was successfully attached to the electrode surface. And finally, when the electrode was associated with ECL-tagged signal aptamer, $R_{et}$ value decreased a little surprisingly (Fig. 4e). Generally, negative charged aptamer repels the negative charged redox probe $[Fe(CN)_6]^{3-/4-}$ and thus the interfacial electron transfer resistance will increase [45–47]. But when the aptamer was labeled with $Ru(bpy)_3^{2+}$ NHS ester that carries two units of positive charges, which will counteract the negative backbone of aptamer. In turn, the association of $Ru(bpy)_3^{2+}$ NHS ester-labeled aptamer to the electrode enhanced the electron transfer of probe ions from the bulk electrolyte solution to the electrode surface to some extent. So, $R_{et}$ value decreased a little. The entire EIS data indicated that the blocking and acceleration effects on electron transfer of ITO electrode were not efficient and remarkable as that of Au electrode [48], and the results were consistent with other published work [45,48–50].

### 3.5. *ECL detection*

The ECL responses of the modified ITO electrodes associated with different concentrations of thrombin were measured after they were immersed in a 50-mM TPA-containing electrolyte solution and exerted a sweep potential from 0 to 1.3 V. The plot of ECL intensity vs. thrombin concentration was well demonstrated in Fig. 5. We investigated the concentrations of standard thrombin solution from 56 nM to 900 nM. And we found the ECL responses for different concentrations of thrombin increased with the increase of thrombin concentration as shown in the inset, which could be used to quantify the thrombin concentration. Further data analysis showed the relationship between ECL intensity and thrombin concentration was a typical behavior of sandwich assay, which was consistent with a published paper [51].

The plot was simulated with a non-linear regression by using the well-known Sigmoidal (Boltzmann) fit which equation is $y = A_2 + (A_1 - A_2)/(1 + \exp((x - x_0)/dx))$; where "$A_2$" is the y value of the bottom plateau of the curve, "$A_1$" is the y value of the top plateau of the curve, $x_0$ is the thrombin concentration to generate half of $(A_1 + A_2)$ ECL signal, and x is thrombin concentration. The plot was well fitted with this equation

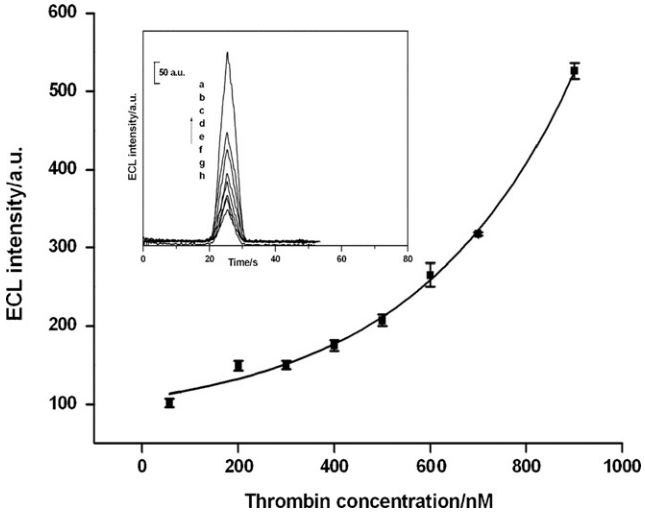


**Fig. 5 – Calibration curves of response-to-dose for thrombin with Sigmoidal (Boltzmann) regression. ECL responses for different concentrations of thrombin were given in the inset. (a) 56 nM, (b) 200 nM, (c) 300 nM, (d) 400 nM, (e) 500 nM, (f) 600 nM, (g) 700 nM, and (h) 900 nM. The error bars represent R.S.D.s of four replicate experiments.**

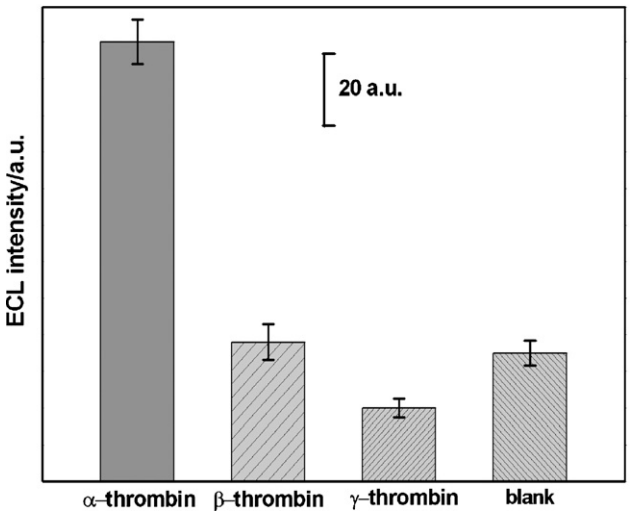


**Fig. 6 – Investigation of the specificity of the ECL aptasensor to the target α-thrombin by comparing with β- and γ-thrombins as negative control and with the blank experiment. The concentration of α-thrombin was 400 nM and the concentration of β- and γ-thrombins was ~800 nM. The error bars indicate R.S.D.s of four replicate experiments.**

and the correlation coefficient value was calculated to be 0.996.

Four repetitions of each standard thrombin solution were carried out to evaluate the reproducibility and precision of the method. The results were reflected by the error bars in Fig. 5. These small R.S.D. values indicated a good analytical performance of the present protocol in terms of reproducibility and accuracy. The detection limit of this assay was determined by measuring the minimum concentration of target thrombin reliably being distinguished from the blank not containing thrombin. In this case, the detection limit was estimated to be 10 nM.

### 3.6. *Detection specificity*

Human α-thrombin is an enzyme protease involved in the coagulation cascade and plays a crucial role in a number of cardiovascular diseases and in blood coagulation and hemostasis process [51]. Human β-thrombin and γ-thrombin are converted products of α-thrombin by enzymatic cleavage or autolytic cleavage that have no physiological function and exhibit a badly reduced clotting activity compared to α-thrombin [52]. In order to evaluate the binding specificity of the ECL aptasensor to its target α-thrombin, we performed a series of contrast experiments using β- and γ-thrombins as negative control and an electrolyte solution without thrombin as blank experiment. The concentrations of control proteins were two fold of α-thrombin. As shown in Fig. 6, α-thrombin revealed much stronger response than β- and γ-thrombins, while the other two converted proteins only showed similar signals to the blank, even γ-thrombin exhibited a signal lower than the blank. It is suggested that the present ECL aptasensor responded to its target α-thrombin with good specificity while other forms of thrombin have almost negligible effect on the detection of α-thrombin, which further validates the aptamer, a promising biorecognition element in biosensor development in virtue of its excellent specificity to the target.

## 4. Conclusion

An aptamer-based sandwich format was proposed to detect the target α-thrombin while other forms of thrombin had a negligible effect on its detection which guaranteed the high specificity of the aptasensor. It also confirmed β- and γ-thrombins have no physiological function and exhibit a greatly reduced bioactivity compared to α-thrombin.

A sensitive enhancement was achieved by AuNPs amplification technique, which simplified the assembly procedure to the ITO electrode surface compared to other method such as glutaraldehyde cross-linking method. The reason why we chose ITO as assembly substrate is owing to its excellent compatibility with microfabrication and miniaturization, plus electrochemical detection system is suitable for the fabrication of microarrays [20], definitely including ECL detection method. In the present work, we employed a simple but subtle miniaturization method in the assembly process, which further facilitated the whole assembly procedure, and saved much expensive biological reagents. This smart sensor fabrication art along with the self-synthesized ECL label together accomplished the cost-effective objective of protein detection. Furthermore, it elucidates the feasibility of fabrication of ECL aptasensor coupled with microarrays. From a long-term perspective, the ECL aptasensor system would be a valuable approach for microarray proteome analysis.

## Acknowledgements

The work was supported by the National Natural Science Foundation of China with grant numbers of 20675078, 20735003, and 90713022 and the 973 Project 2007CB714500 as well as Chinese Academy of Sciences Project KJCX2 YWHO9.

## REFERENCES

[1] J. Wang, Anal. Chim. Acta 469 (2002) 63.
[2] X.-B. Yin, B. Qi, X. Sun, X. Yang, E. Wang, Anal. Chem. 77 (2005) 3525.
[3] C.-C. Huang, Z. Cao, H.-T. Chang, W. Tan, Anal. Chem. 76 (2004) 6973.
[4] K.A. Davis, Y. Lin, B. Abrams, S.D. Jayasena, Nucleic Acids Res. 26 (1998) 3915.
[5] F. Kleinjung, S. Klussmann, V.A. Erdmann, F.W. Scheller, J.P. Fürste, F.F. Bier, Anal. Chem. 70 (1998) 328.
[6] R.A. Potyrailo, R.C. Conrad, A.D. Ellington, G.M. Hieftje, Anal. Chem. 70 (1998) 3419.
[7] E. Baldrich, A. Restrepo, C.K. O'Sullivan, Anal. Chem. 76 (2004) 7053.
[8] P.L. Sazani, R. Larralde, J.W. Szostak, J. Am. Chem. Soc. 126 (2004) 8370.
[9] B.R. Baker, R.Y. Lai, M.S. Wood, E.H. Doctor, A.J. Heeger, K.W. Plaxco, J. Am. Chem. Soc. 128 (2006) 3138.
[10] R. Kirby, E.J. Cho, B. Gehrke, T. Bayer, Y.S. Park, D.P. Neikirk, J.T. McDevitt, A.D. Ellington, Anal. Chem. 76 (2004) 4066.
[11] H. Wang, M. Lu, X.C. Le, Anal. Chem. 77 (2005) 4985.
[12] M.N. Stojanovic, D.W. Landry, J. Am. Chem. Soc. 124 (2002) 9678.
[13] J.K. Herr, J.E. Smith, C.D. Medley, D. Shangguan, W. Tan, Anal. Chem. 78 (2006) 2918.
[14] Z. Tang, D. Shangguan, K. Wang, H. Shi, K. Sefah, P. Mallikratchy, H.W. Chen, Y. Li, W. Tan, Anal. Chem. 79 (2007) 4900.
[15] M. Liss, B. Petersen, H. Wolf, E. Prohaska, Anal. Chem. 74 (2002) 4488.
[16] T.G. Mccauley, N. Hamaguchi, M. Stanton, Anal. Biochem. 319 (2003) 244.
[17] S. Nagatoishi, Y. Tanaka, K. Tsumoto, Biochem. Biophys. Res. Commun. 352 (2007) 812.
[18] A.-E. Radi, C.K. O'Sullivan, Chem. Commun. (2006) 3432.
[19] Y. Xiao, A.A. Lubin, A.J. Heeger, K.W. Plaxco, Angew. Chem. Int. Ed. 44 (2005) 5456.
[20] K. Ikebukuro, C. Kiyohara, K. Sode, Biosens. Bioelectron. 20 (2005) 2168.
[21] X. Fang, Z. Cao, T. Beck, W. Tan, Anal. Chem. 73 (2001) 5752.
[22] H. Wei, B. Li, J. Li, E. Wang, S. Dong, Chem. Commun. (2007) 3735.
[23] B. Basnar, R. Elnathan, I. Willner, Anal. Chem. 78 (2006) 3638.
[24] Y. Li, H.J. Lee, R.M. Corn, Nucleic Acids Res. 34 (2006) 6416.
[25] M.M. Richter, Chem. Rev. 104 (2004) 3003.
[26] K.A. Fähnrich, M. Pravda, G.G. Guilbault, Talanta 54 (2001) 531.
[27] G.F. Blackburn, H.P. Shah, J.H. Kenten, J. Leland, R.A. Kamin, J. Link, J. Peterman, M.J. Powell, A. Shah, D.B. Talley, S.K. Tyagi, E. Wilkins, T.-G. Wu, R.J. Massey, Clin. Chem. 37 (1991) 1534.
[28] J.H. Kenten, S. Gudibande, J. Link, J.J. Wiley, B. Curfman, E.O. Major, R.J. Massey, Clin. Chem. 38 (1992) 873.
[29] W. Miao, A.J. Bard, Anal. Chem. 75 (2003) 5825.
[30] W. Miao, A.J. Bard, Anal. Chem. 76 (2004) 5379.
[31] Y. Li, H. Qi, Y. Peng, Q. Gao, C. Zhang, Electrochem. Commun. 10 (2008) 1322.
[32] Y. Li, H. Qi, Y. Peng, J. Yang, C. Zhang, Electrochem. Commun. 9 (2007) 2571.
[33] X. Li, L. Shen, D. Zhang, H. Qi, Q. Gao, C. Zhang, Biosens. Bioelectron. 23 (2008) 1624.
[34] X. Wang, J. Zhou, W. Yun, S. Xiao, Z. Chang, P. He, Y. Fang, Anal. Chim. Acta 598 (2007) 242.
[35] X. Wang, W. Yun, J. Zhou, P. Dong, P. He, Y. Fang, Chin. J. Chem. 26 (2008) 315.
[36] L. Wang, C. Yang, W. Tan, Nano Lett. 5 (2005) 37.
[37] K.C. Grabar, R.G. Freeman, M.B. Hommer, M.J. Natan, Anal. Chem. 67 (1995) 735.
[38] J.J. Storhoff, R. Elghanian, R.C. Mucic, C.A. Mirkin, R.L. Letsinger, J. Am. Chem. Soc. 120 (1998) 1959.
[39] L. Fang, Z. Lü, H. Wei, E. Wang, Biosens. Bioelectron. 23 (2008) 1645.
[40] A.-M. Spehar-Deleze, L. Schmidt, R. Neier, S. Kulmala, N. Rooij, M. Koudelka-Hep, Biosens. Bioelectron. 22 (2006) 722.
[41] T.M.-H. Lee, L.-L. Li, I.-M. Hsing, Langmuir 19 (2003) 4338.
[42] P. He, L. Shen, Y. Cao, D. Li, Anal. Chem. 79 (2007) 8024.
[43] S. Zhang, N. Wang, H. Yu, Y. Niu, C. Sun, Bioelectrochemistry 67 (2005) 15.
[44] A.N. Asanov, W.W. Wilson, P.B. Oldham, Anal. Chem. 70 (1998) 1156.
[45] M. Zayats, Y. Huang, R. Gill, C. Ma, I. Willner, J. Am. Chem. Soc. 128 (2006) 13666.
[46] A.-E. Radi, J.L.A. Sánchez, E. Baldrich, C.K. O'Sullivan, Anal. Chem. 77 (2005) 6320.
[47] N. de-los-Santos-Álvarez, M.J. Lobo-Castañó, A.J. Miranda-Ordieres, P. Tuñón-Blanco, J. Am. Chem. Soc. 129 (2007) 3808.
[48] C. Ruan, L. Yang, Y. Li, Anal. Chem. 74 (2002) 4814.
[49] L. Yang, Y. Li, Biosens. Bioelectron. 20 (2005) 1407.
[50] Y. Wang, W. Qian, Y. Tan, S. Ding, H. Zhang, Talanta 72 (2007) 1134.
[51] S. Centi, S. Tombelli, M. Minunni, M. Mascini, Anal. Chem. 79 (2007) 1466.
[52] G. Karlsson, Protein Exp. Purif. 27 (2003) 171.